SUPPORTING INFORMATION

Temperature-driven Isosymmetric Reversible Phase Transition in the Hormone Estradiol 17β Valerate

Javier Ellena,[†*] *Karina de Paula,*[†] *Cristiane C. de Melo,*[†] *Cecília C. P. da Silva,*[†] *Beatriz P. Bezerra,*[††] *Tiago Venâncio,*[†††] *Alejandro P. Ayala*[††*]

[†] Instituto de Física de São Carlos, Universidade de São Paulo, CP 369, 13560-970, São Carlos, SP, Brazil; [††] Departamento de Física, Universidade Federal do Ceará, CP 6030, Fortaleza, Ceará 60455–970; [†††] Departamento de Química, Universidade Federal de São Carlos, Cx Postal 676, 13565-905 São Carlos, SP, Brasil; * e-mail: javiere@ifsc.usp.br

Intra and Intermolecular Interactions

Table S1 - Geometrical parameters characterizing the intra and intermolecular interactions of E2V at both temperatures. The symbols "D" and "A" refers to hydrogen donor and acceptors, respectively.

E2V	Interaction	D…H(Å)	D...A(Å)	H...A(Å)	D-H...A(º)	Symmetry code
			298K			
Conformer A	O1A–H1•••O3A	0.70	2.770(6)	2.08	171	x, y, z+1
	C16A–H16B•••O2A	0.80	2.517(7)	2.15	108	intramolecular
Conformer B	O1B–H2•••O3B	0.81	2.799(6)	1.99	171	x, y, z-1
			100.0(2)K			
Conformer A	O1A–H1•••O3A	0.93	2.793(2)	1.87	171	x, y, -1+z
Conformer B	O1B–H2•••O3B	0.82	2.780(3)	2.00	158	1+x, y, -1+z
	C14B–H14•••*Cg*1	1.00	2.818(4)	1.790	174.99	-x,-y+1,-z+2

*Cg*1 represents the centroid of the phenyl ring: C1A-C2A-C3A-C4A-C5A-C10A.

X-ray Powder Diffraction

For comparison, Figure S1 shows the theoretical X-ray powder diffraction pattern of E2V calculated from the single crystal x-ray diffraction experiment at room temperature and 100 K using the MERCURY program and the experimental powder diffractogram at similar

temperatures. Both, experimental and calculated PXRD diagrams can be satisfactorily compared. All peaks form the experimental PXRD pattern overlaid to those observed in the simulated X-ray diffractogram showing that the E2V sample has no extra crystalline phase thus proving the purity of the sample. Also, since no broad hump from amorphous material was observed the powdered sample is completely crystalline. Table S2 lists the most intense reflections of the calculated powder patterns.

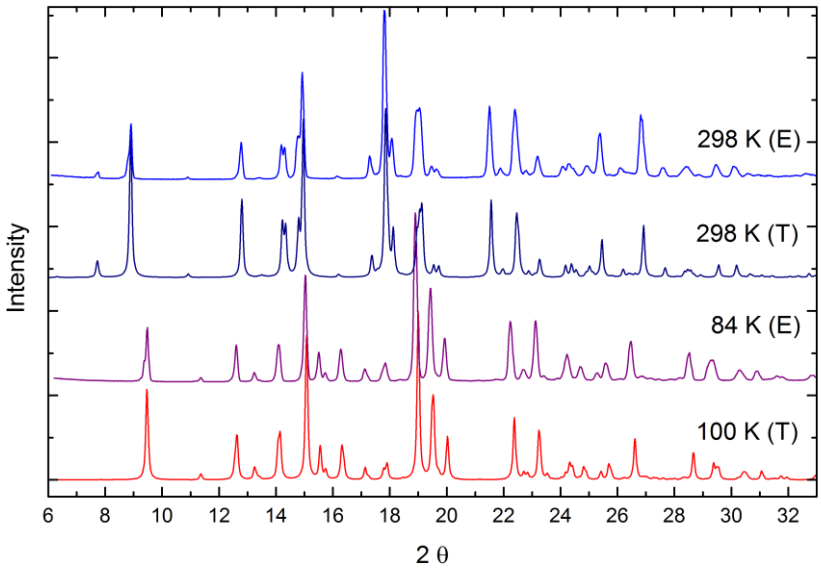

Figure S1. Theoretical (T) and experimental (T) PXRD patterns of E2V at room and low temperature.

Table S2 – Relative intensity of the most intense reflections of the calculated powder patterns.

100 K		298 K	
d [Å]	I/I_{max} [%]	d [Å]	I/I_{max} [%]
9.331	54	11.442	8
7.008	33	9.928	71
6.672	9	6.910	39
6.267	42	6.223	25
5.870	85	6.171	25
5.694	20	5.985	26
5.424	27	5.917	77
5.169	7	5.101	12
4.984	5	4.962	100
4.951	9	4.892	27
4.667	100	4.650	83
4.544	69	4.498	5
4.431	26	4.118	39
3.969	39	4.042	5
3.823	34	3.954	46
3.654	20	3.821	10
3.583	10	3.678	5
3.462	12	3.648	6
3.347	25	3.556	9
3.111	16	3.497	18
3.038	8	3.310	25
3.023	11	3.130	10
2.932	10	3.020	6

Thermal analysis and Spectroscopic Characterization at room temperature.

Figure S2 shows the DSC and TGA curves of E2V above room temperature. The high temperature DSC show the presence of an endothermic peak with onset temperature around 145°C associated with the melting of the material. TGA shows that the decomposition process of the sample starts 262°C.

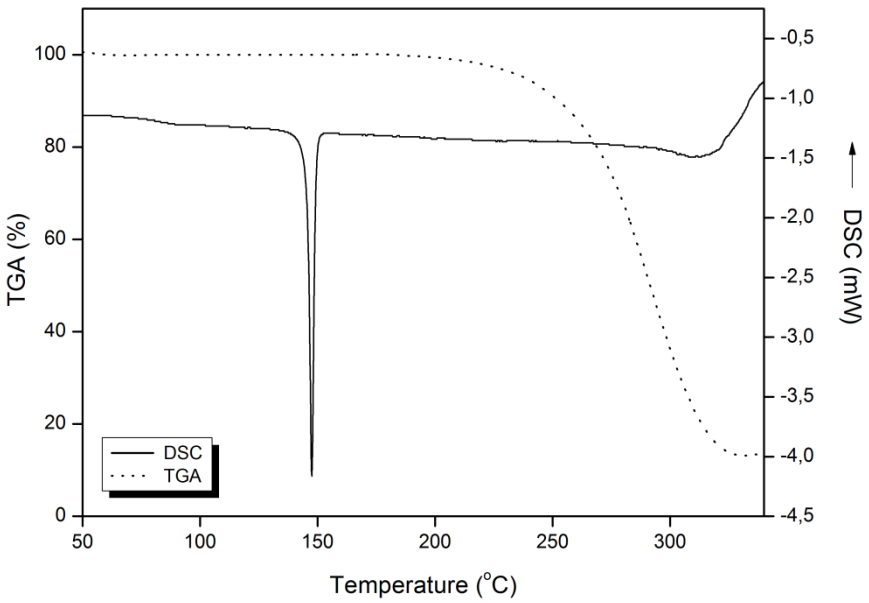

Figure S2. DSC and TGA Curves of E2V above room temperature.

Vibrational spectroscopy

The room temperature infrared and Raman spectra of E2V are presented in Figure S3. The observed bands were divided into regions to facilitate the description.

High Region (2800-3600cm^{-1}): In this region, we can verify the presence of the OH stretching vibrations. The OH mode of the group involving in the intermolecular hydrogen bond is observed in 3400-3200 cm^{-1} characterized as wide and strong in IR and weak in Raman. Besides these bands some Raman modes appear between 2990cm^{-1} to 3040cm^{-1}

related to the sp^2 aromatics carbons. The modes related to the sp^3 carbons atoms appear just below, between 2990cm^{-1} to 2800cm^{-1}.

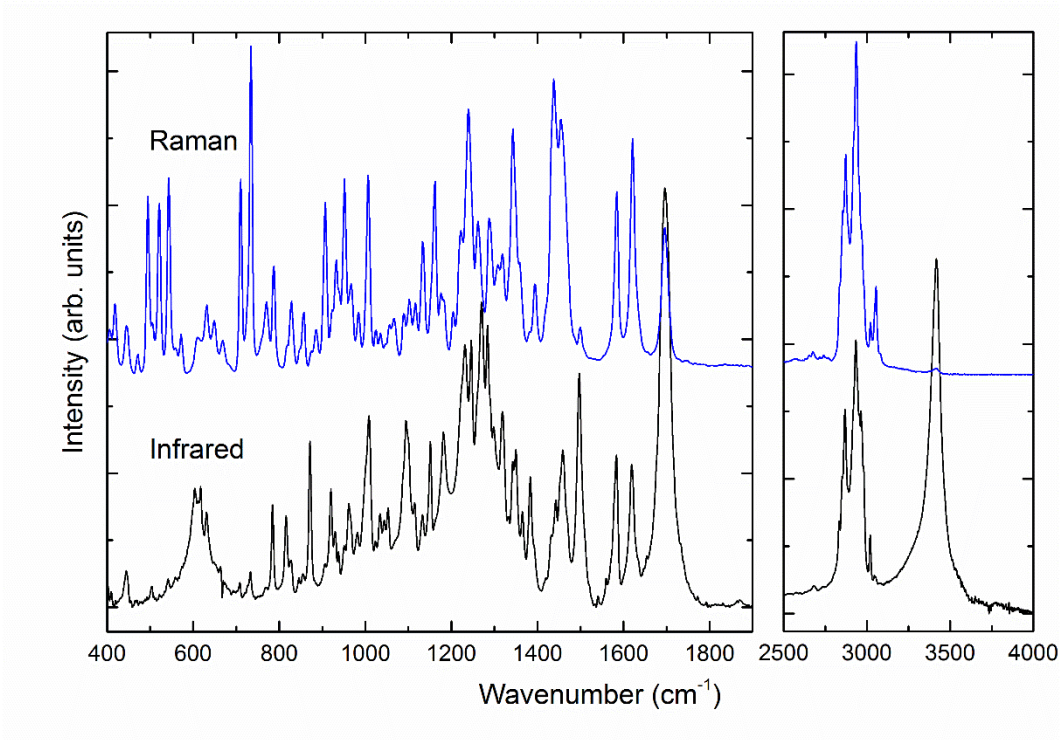

Figure S3. Infrared and Raman spectra of E2V at room temperature.

Average energy region (1150-1700cm^{-1}): In this region observed medium to weak bands around 1740 cm^{-1} in the Raman spectrum which may correspond to the C=O stretching of the ester group. In the 1410-1310 cm^{-1} range appears characteristic bands of the phenol group. Furthermore, the stretching band at 1275-1185 cm^{-1} it may be attributed to the asymmetric mode of the COC group.

Low Energy region (400-1100 cm^{-1}): In this region the symmetric stretching modes of the ester COC can be identified between 1150 and 1160 cm^{-1} which are weak in the Raman. This region encompasses also other characteristic modes of phenol in the 720-600 cm^{-1} regions and 450-375 cm^{-1}. The first one refers to the OH out of plane vibrations, that is

medium to weak, and the second involves vibrations in the plane, in which case the bands appear in the Raman as weak.

Superposition of Molecules in the Asymmetric Unit

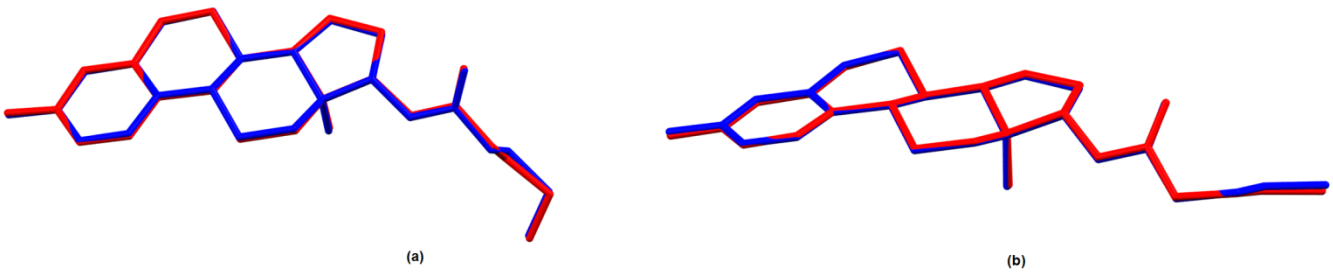

Figure S4. Superposition of conformers A in red and B in blue at (a) room temperature and (b) low temperature.

NMR

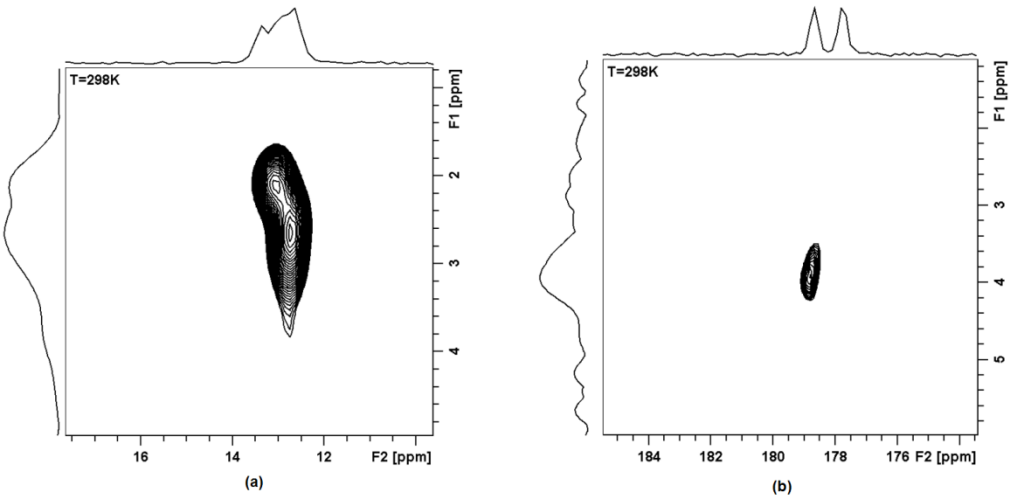

Figure S5. 2D ^{1}H-^{13}C FSLG-HETCOR correlation map for E2V at 298K: **(a)** expansion of methyl groups (C18 and C23); **(b)** expansion of carbonyl group C19.

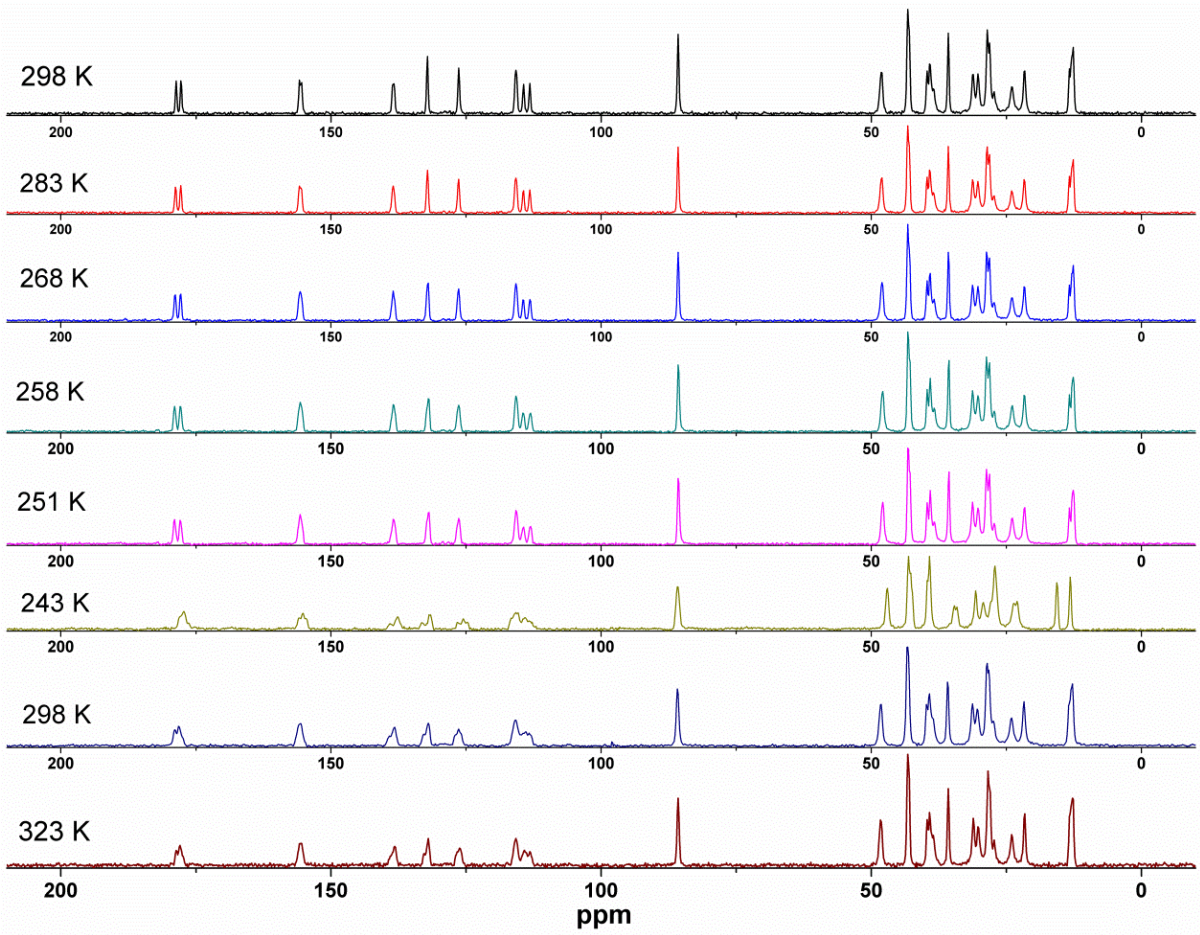

Figure S6. ^{13}C solid state NMR spectra for E2V at different temperatures.

Low Temperature IR spectra

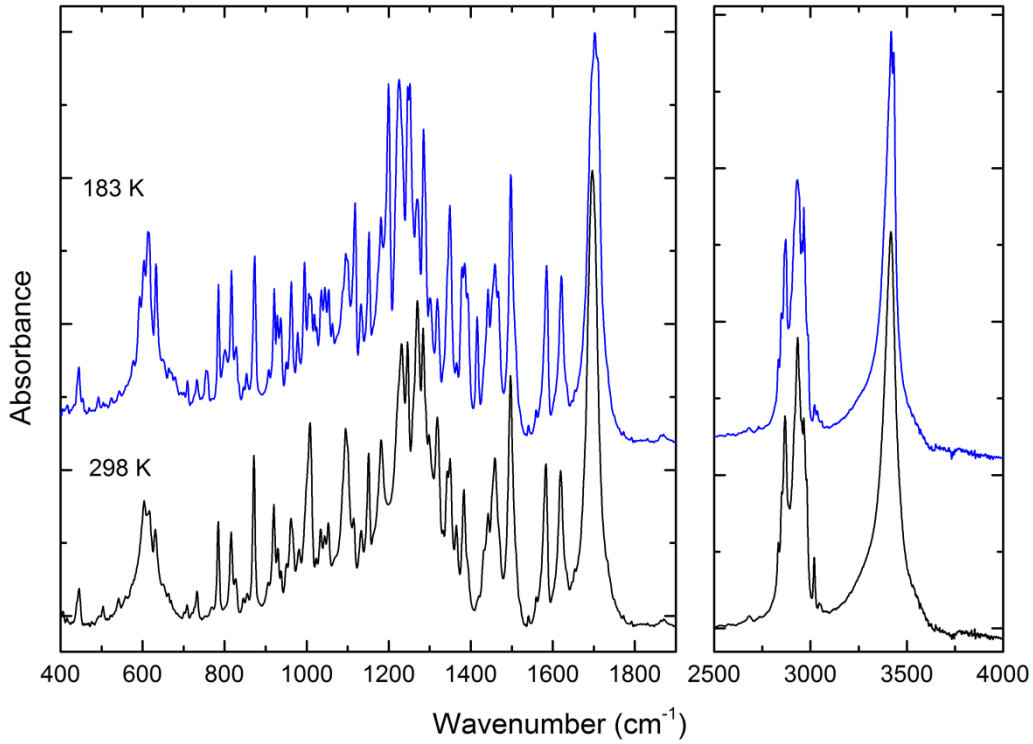

Figure S7. Comparison of the room and low temperature infrared spectra.

Quantum Mechanical Calculations

The electronic structure and optimized geometry of the molecule were computed by *ab initio* DFT using Gaussian 09 program package employing 6-31++G(d,p) basis set based on Backe's three-parameter hybrid exchange functional with Lee-Yang-Parr correlation functional (B3LYP). The basis set 6-311++G(d,p) augmented by d polarization functions on heavy atoms and p polarization functions on hydrogen atoms as well as diffuse functions for both hydrogen and heavy atoms were used for better description of polar bonds C=O and CH_2 groups. The optimized structural parameters were used to calculate the absolute infrared absorption intensities in the harmonic approximation at the DFT level. The positive values of all the obtained wavenumbers confirm the stability of optimized geometry.

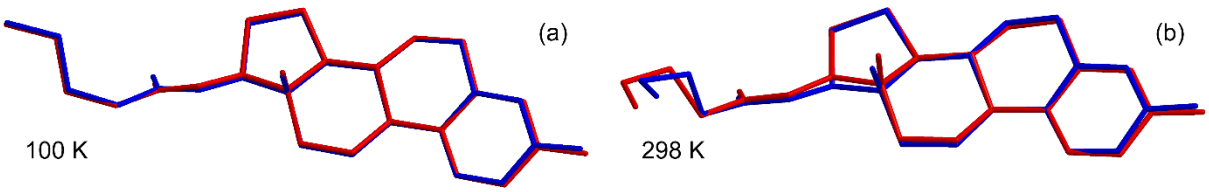

Figure S8. Comparison experimental (red) and calculated (blue) molecular conformations of the (a) low and (b) room temperature crystalline structures.